Baustatik – Baupraxis 15, © 2024, Technische Universität Hamburg

Computational modeling of fiber orientation during 3D-concrete-printing

Koussay Daadouch[1], **Janis Reinold**[1,2], **Vladislav Gudžulić**[1], **Günther Meschke**[1]

[1]*Institute for Structural Mechanics, Ruhr University Bochum*
[2]*South Westphalia University of Applied Sciences*

Abstract: In 3D printing of fiber-reinforced concrete, fibers naturally align with the printing direction due to material shearing, enabling a certain degree of control over fiber orientation in component production. This contribution introduces an innovative integration of the Folgar-Tucker fiber orientation model into a fluid dynamics framework using the Particle Finite Element Method for simulating fiber orientation changes during 3D concrete printing. The fiber orientation state is characterized using a second-order orientation tensor, and an anisotropic Bingham model for the viscous fiber-concrete mixture describes fluid constitutive behavior. The model is validated by a comparison of the simulated orientation states a 3D-printed concrete layer, varying the extrusion nozzle diameters, with experimental data from the literature. Additionally, we conduct various parametric studies to investigate the flow dynamics, fiber realignment mechanisms, and the impact of process parameters on the fiber orientation within printed components.

1 Introduction

In recent years, automated construction methods like additive manufacturing with fresh concrete have rapidly advanced, with 3D concrete printing, in particular, gaining notable momentum. This technology involves the automated layer-by-layer deposition of firm fresh concrete through an extrusion nozzle to create structures without traditional formwork. One of the main challenges in this field is the incorporation of reinforcement [10, 11]. Fiber-reinforced concrete has emerged as a practical solution that addresses this challenge. Experimental studies have shown that fibers align themselves with the printing direction during 3D concrete printing [6, 15]. Moreover, the degree of fiber orientation can be controlled by adjusting process parameters, such as flow rate or printing speed, during printing [2]. Accurately predicting fiber orientation within printed components is crucial for ensuring a reliable printing

process. Given the complexity of the process and material parameters, along with intricate flow mechanisms, such predictions are challenging and require comprehensive experimental and numerical investigations. In this context, we introduce a numerical approach based on the Particle Finite Element Method (PFEM) [7, 13] and a fiber orientation model by Folgar and Tucker [4]. This approach enables the analysis of the extrusion process in fiber-reinforced 3D concrete printing.

This contribution summarizes the work presented in detail in [17], in which we adopt a PFEM-based model that utilizes the Folgar-Tucker fiber orientation model to simulate the concrete 3D printing process. This model describes the evolving orientation state of a group of fibers using a second-order orientation tensor [1, 5, 17]. We introduce this approach to investigate the extrusion process during fiber-reinforced 3D concrete printing with the aim of examining the effect of process parameters on the fiber alignment.

2 Fiber orientation model

The orientation of a single fiber can be characterized by the unit vector $\boldsymbol{p}$ which points in the fiber direction and is defined as:

$$\boldsymbol{p} = [\sin(\theta)\cos(\phi),\ \sin(\theta)\sin(\phi),\ \cos(\theta)]^T, \tag{1}$$

with the azimuth angle ϕ and the polar angle θ. Jeffery introduced a model for the flow of a single fiber within a Newtonian fluid [8]. Subsequently, Folgar and Tucker extended Jeffery's framework to account for a group of fibers by recasting the governing equations into a probabilistic Fokker-Planck type of equation, where the fiber-fiber interactions are modeled by adding a diffusivity term [4]. The governing equation for evolution of the fiber orientation distribution function $\psi(\theta, \phi)$ proposed by Folgar and Tucker [4] is given as [1]:

$$\dot{\psi} = -\nabla_i^S(\psi \underbrace{(W_{ij}p_j + \lambda(D_{ij}p_j - D_{kl}p_k p_l p_i))}_{=\dot{p}_i^h} \underbrace{-C_I|\dot{\gamma}|\nabla_i^S\psi}_{=q_i^h}), \tag{2}$$

where ∇^S is the gradient operator in orientation space, $D_{ij} = \frac{1}{2}\left(\frac{\partial v_i}{\partial x_j} + \frac{\partial v_j}{\partial x_i}\right)$ is the strain tensor, $W_{ij} = \frac{1}{2}\left(\frac{\partial v_i}{\partial x_j} - \frac{\partial v_j}{\partial x_i}\right)$ is the spin tensor, and $|\dot{\gamma}| = \sqrt{2D_{ij}D_{ij}}$ the equivalent strain rate. The shape factor λ, and the isotropic rotary diffusivity factor C_I depend on the fibers aspect ratio [17]. The hydrodynamic contribution $\dot{\boldsymbol{p}}^h$ is the evolution law for the motion of a single spheroidal particle suspended in a Newtonian fluid [8], while $\boldsymbol{q}^h$ is a phenomenological diffusivity term, which accounts for the interactions between fibers [4].

Solving Eq. (2) directly to obtain the orientation distribution function is computationally demanding. Instead, it has been observed that computing moments of the distribution function is much more computationally efficient and adequately precise for most practical purposes [1]. These moments, known as orientation tensors of order n, serve as analogs to moments of a linear distribution function, including the first moment (expected value) and second moment (variance). It's important to note that odd-ordered moments of a symmetric orientation

distribution function on the unit sphere are zero, and therefore, only even moments are calculated. For typical applications, considering second and fourth order orientation tensors will suffice. These tensors are defined as follows:

$$a_{2,ij} = \int_{\mathbb{S}} p_i p_j \psi \, d\mathbb{S} = \int_{\phi=0}^{2\pi} \int_{\theta=0}^{\pi} p_i p_j \psi \sin(\theta) \, d\theta \, d\phi, \tag{3}$$

$$a_{4,ijkl} = \int_{\mathbb{S}} p_i p_j p_k p_l \psi \, d\mathbb{S} = \int_{\phi=0}^{2\pi} \int_{\theta=0}^{\pi} p_i p_j p_k p_l \psi \sin(\theta) \, d\theta \, d\phi. \tag{4}$$

3 Constitutive model for fresh concrete flow including fibers

When fibers are introduced into a fresh concrete mix, they increase the likelihood of collisions among solid particles. Consequently, this leads to an increase in the viscosity and yield stress of the mixture. Furthermore, the suspension exhibits an anisotropic response, primarily because the fibers reorient themselves during flow [9]. This anisotropy is observable through amplified elongational viscosities in the fiber direction and the occurrence of shear-thinning effects [14]. Sommer et al. introduced a constitutive model for anisotropic fiber suspensions [3, 18]. In this approach, a transversely anisotropic fluid model is volume-averaged following the method described in [1], utilizing second and fourth-order orientation tensors. As outlined in [3, 18], assuming equal values for the in-plane and transverse shear viscosities and employing the regularized Bingham model, the deviatoric Cauchy stress tensor for the fiber suspension can be defined as:

$$\begin{aligned} \tau_{ij} = \mu_{ijkl} D_{kl} = & \Bigg[4\eta_{23}(R_\eta - 1) \left[a_{4,ijkl} - \frac{1}{3} \left(a_{2,ij}\delta_{kl} + a_{2,kl}\delta_{ij} - \frac{1}{3}\delta_{ij}\delta_{kl} \right) \right] \\ & + 2\eta_{23} \, I^d_{ijkl} + 2\frac{\tau_0}{|\dot{\gamma}|} \left(1 - e^{-m|\dot{\gamma}|} \right) I^d_{ijkl} \Bigg] D_{kl}, \end{aligned} \tag{5}$$

where μ_{ijkl} is the fourth order viscosity tensor, η_{23} is the transverse shear viscosity and R_η is an anisotropy ratio, which equals to one if there are no fibers. Constitutive assumptions based on the fiber volume fraction for τ_0, η_{23} and R_η are summarized in [17].

4 Numerical solution procedure

In this work, flowing fiber-reinforced concrete is modeled as a homogeneous material.

To solve the balance equations, the Particle Finite Element Method (PFEM) is utilized, which is a variant of the Finite Element Method implemented within an updated Lagrangian framework [7, 13]. The discretization of the spatial domain is carried out using standard low-order simplex elements, applicable in both 2D and 3D contexts. Additional details regarding the solution procedure can be found in [17]. While the original re-meshing procedure in PFEM previously involved the application of a Delaunay tessellation on the particles (nodes) along

with a free surface reconstruction method based on the alpha shape technique, the re-meshing strategy employed in this study has been improved by employing a constrained Delaunay tessellation to minimize changes to the free surface [16, 17].

5 Numerical analysis of the extrusion process

The numerical simulation focused exclusively on modeling a portion of the extrusion nozzle. To simplify the simulation and facilitate a more generalized analysis of various nozzle geometries, the simulation excluded the modeling of fresh concrete flow and fiber orientation within the extruder. Additionally, only straight, circular extrusion nozzles were considered.

The geometry, spatial disretization and boundary conditions of the model are shown in Fig. 1. More information can be found in [17].

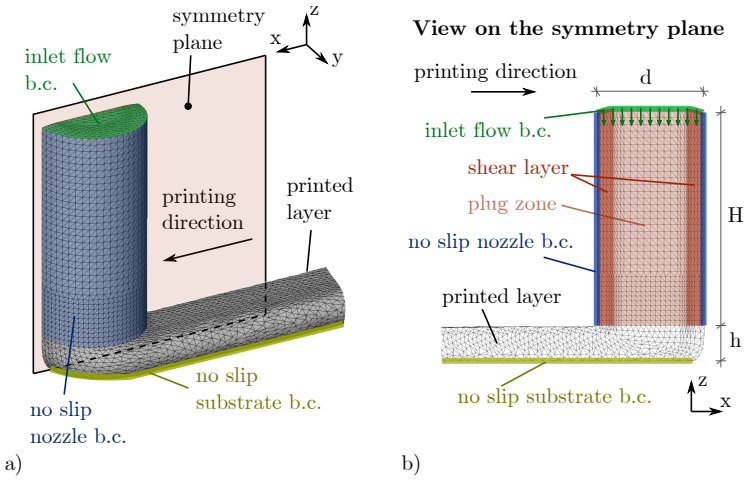

Figure 1: Geometry, numerical discretization, and boundary conditions of the 3D-concrete-printing extrusion process simulations in the vicinity of the extrusion nozzle: Side view a) and view on the symmetry plane b). (Reproduced from [17])

The material and fiber flow properties were chosen as $\tilde{\mu} = 10$ Pa s, $\tilde{\tau}_0 = 28.4024$ Pa, $\phi_s = 0.45$, $\rho = 2100$ kg/m^3, $c = 0.01$, $r = 30$, and $\kappa = 0.2$ (yielding $\mu = 10$ Pa s and $\tau_0 = 300$ Pa when $c = 0$), which were assumed based on typical values found in the literature [2, 12, 16]. The time step size was specified as $\Delta t = 0.004$ s, and layers of 50 cm length were printed. The simulated fiber orientation state is depicted in Fig. 2a) and Fig. 2b) shows the fiber orientation along the symmetry plane.

To validate and further explore the printed cross-section, it was divided into two segments: Section A (where $y > d/4$) and Section B (where $y < d/4$), as illustrated in Figure 2c. To understand the alignment of fibers, we introduce the orientation number N_o [17]. This parameter quantifies the degree of fiber alignment in the printing direction. It tends towards zero when there are only a few fibers aligned with the printing direction and approaches one when all fibers are oriented in the printing direction. Figure 2d shows the averaged

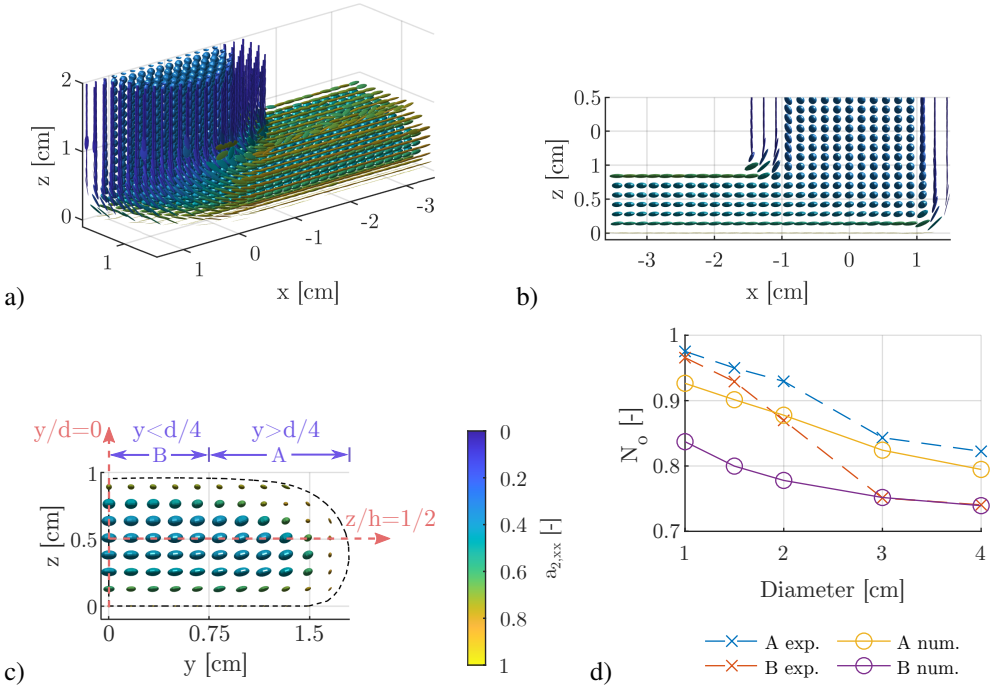

Figure 2: 3D-printing of fiber-reinforced concrete: The orientation tensor is visualized as an ellipsoid and color coding corresponds to the orientation tensor component $a_{2,xx}$. a) A close-up examination of the region near the extrusion nozzle. b) An observation of the symmetry plane surrounding the extrusion nozzle. c) An observation of the printed cross-section, which includes delineations for Sections A ($y > d/4$) and B ($y < d/4$). d) The orientation number, obtained through simulations with different nozzle diameters (d) compared to experimental results from [2]. (Reproduced from [17])

orientation number N_o for Sections A and B, derived from simulations using various nozzle sizes, and it is compared to experimental results reproduced from [2]. Section A exhibits higher orientation numbers than Section B, suggesting a more pronounced fiber alignment in the printing direction (x-direction) at the layer edges, which aligns with prior findings.

An extensive and more comprehensive sensitivity analysis was conducted by the authors in [17] where the effect of different process parameters (nozzle diameter, printing speed, flow rate and printing height) on the fiber alignment is examined.

6 Conclusions

We have introduced a numerical modeling approach for simulating the flow of fresh fiber-reinforced concrete within a Particle Finite Element (PFEM) framework. The model was validated by comparing the simulated fiber orientation states of printed cross-sections from 3D

concrete printing with experimental results from the literature, focusing on various extrusion nozzle diameters. Our computational investigations demonstrate that process parameters can exert some control over fiber orientation in the printing direction during 3D concrete printing process. The results shown here motivate the future research, in particular the exploration of conical extrusion nozzle shapes, multi-layer printing scenarios, and the development of submodels that consider the influence of fiber orientation on yield stress.

References

[1] ADVANI, S. G. ; TUCKER, C. L.: The use of tensors to describe and predict fiber orientation in short fiber composites. In: *Journal of Rheology* 31 (1987), S. 751–784

[2] ARUNOTHAYAN, A. R. ; NEMATOLLAHI, B. ; RANADE, R. ; BONG, S. H. ; SANJAYAN, J. G. ; KHAYAT, K. H.: Fiber orientation effects on ultra-high performance concrete formed by 3D printing. In: *Cement and Concrete Research* 143 (2021), S. 106384

[3] FAVALORO, A. J. ; TSENG, H. C. ; PIPES, R. B.: A new anisotropic viscous constitutive model for composites molding simulation. In: *Composites Part A: Applied Science and Manufacturing* 115 (2018), S. 112–122

[4] FOLGAR, F. ; TUCKER, C. L.: Orientation behavior of fibers in concentrated suspensions. In: *Journal of Reinforced Plastics and Composites* 3 (1984), S. 98–119

[5] GUDZULIC, V. ; DANG, T. ; MESCHKE, G. : Computational modeling of fiber flow during casting of fresh concrete. In: *Computational Mechanics* 63(6) (2018), S. 1111–1129

[6] HUANG, H. ; GAO, X. ; TENG, L. : Fiber alignment and its effect on mechanical properties of UHPC: An overview. In: *Construction and Building Materials* 296 (2021), S. 123741

[7] IDELSOHN, S. R. ; OÑATE, E. ; DEL PIN, F. : The particle finite element method: a powerful tool to solve incompressible flows with free-surfaces and breaking waves. In: *International Journal for Numerical Methods in Engineering* 61 (2004), Nr. 7, S. 964–989

[8] JEFFERY, G. B. ; FILON, L. N. P.: The motion of ellipsoidal particles immersed in a viscous fluid. In: *Proceedings of the Royal Society of London. Series A, Containing Papers of a Mathematical and Physical Character* 102 (1922), Nr. 715, S. 161–179

[9] MARTINIE, L. ; ROSSI, P. ; ROUSSEL, N. : Rheology of fiber reinforced cementitious materials: classification and prediction. In: *Cement and Concrete Research* 40 (2010), Nr. 2, S. 226–234

[10] MECHTCHERINE, V. ; BOS, F. P. ; PERROT, A. ; LEAL DA SILVA, W. R. ; NERELLA, V. N. ; FATAEI, S. ; ET AL.: Extrusion-based additive manufacturing with cement-based materials - Production steps, processes, and their underlying physics: A review. In: *Cement and Concrete Research* 132 (2020), S. Article 106037

[11] MECHTCHERINE, V. ; BUSWELL, R. ; KLOFT, H. ; BOS, F. P. ; HACK, N. ; WOLFS, R. ; SANJAYAN, J. ; NEMATOLLAHI, B. ; IVANIUK, E. ; NEEF, T. : Integrating reinforcement in digital fabrication with concrete: A review and classification framework. In: *Cement and Concrete Composites* 119 (2021), S. 103964

[12] MOHAN, M. K. ; RAHUL, A. V. ; VAN TITTELBOOM, K. ; DE SCHUTTER, G. : Rheological and pumping behaviour of 3D printable cementitious materials with varying aggregate content. In: *Cement and Concrete Research* 139 (2021), S. Article 106258

[13] OÑATE, E. ; IDELSOHN, S. R. ; DEL PIN, F. ; AUBRY, R. : The particle finite element method: an overview. In: *International Journal of Computational Methods* 1 (2004), Nr. 02, S. 267–307

[14] PETRIE, C. J. S.: The rheology of fibre suspensions. In: *Journal of Non-Newtonian Fluid Mechanics* 87 (1999), Nr. 2, S. 369–402

[15] PHAM, L. ; TRAN, P. ; SANJAYAN, J. : Steel fibres reinforced 3D printed concrete: Influence of fibre sizes on mechanical performance. In: *Construction and Building Materials* 250 (2020), S. 118785

[16] REINOLD, J. ; MESCHKE, G. : A mixed u-p edge-based Smoothed Particle Finite Element formulation for viscous flow simulations. In: *Computational Mechanics* 69 (2022), S. 891–910

[17] REINOLD, J. ; GUDŽULIĆ, V. ; MESCHKE, G. : Computational modeling of fiber orientation during 3D-concrete-printing. In: *Computational Mechanics* 71 (2023), Nr. 6, S. 1205–1225

[18] SOMMER, D. E. ; FAVALORO, A. J. ; PIPES, R. B.: Coupling anisotropic viscosity and fiber orientation in applications to squeeze flow. In: *Journal of Rheology* 62 (2018), Nr. 3, S. 669–679